

A Decoherence-Free Quantum Memory Using Trapped Ions

D. Kielpinski,^{1*} V. Meyer,¹ M. A. Rowe,¹ C. A. Sackett,¹
W. M. Itano,¹ C. Monroe,² D. J. Wineland¹

We demonstrate a decoherence-free quantum memory of one qubit. By encoding the qubit into the decoherence-free subspace (DFS) of a pair of trapped ⁹Be⁺ ions, we protect the qubit from environment-induced dephasing that limits the storage time of a qubit composed of a single ion. We measured the storage time under ambient conditions and under interaction with an engineered noisy environment and observed that encoding into the DFS increases the storage time by up to an order of magnitude. The encoding reversibly transfers an arbitrary qubit stored in a single ion to the DFS of two ions.

A quantum memory stores information in superposition states of a collection of two-level systems called “qubits.” Quantum computation, which may provide a substantial speedup in factoring large numbers (1) and in searching databases (2), works by operating on information in the form of such superpositions. Robust quantum memories are therefore essential to realizing the potential gains of quantum computing (3). However, interaction of a quantum memory with its environment destroys the stored information, a process called “decoherence” (4, 5). Many proposed quantum memories decohere because of an environment that has the same coupling to each qubit (6–12). Encoding the stored information into a decoherence-free subspace, or DFS, allows the memory to retain information, even in the presence of this type of decoherence (10–12). The DFS states are invariant under the coupling to such an environment, protecting the encoded “logical qubit” from the decoherence affecting general superpositions of the “physical qubits” that make up the full state space. DFSs have been shown to require an asymptotically small overhead for large systems (10) and to support universal fault-tolerant quantum logic (13, 14). These properties suggest that DFSs will be intrinsic to future quantum computing architectures. Logic gates on DFS-encoded qubits have been proposed in the context of cavity quantum electrodynamics (15) and solid state quantum logic schemes (14). Also, a recent experiment has demonstrated the immunity of a DFS of two photons to collective noise (16). Here we demonstrate the immunity of a DFS of two atoms to collective dephasing and implement a technique for encoding an arbitrary physical qubit state into the DFS.

Our physical qubits are ⁹Be⁺ ions confined along the axis of a miniature linear radio-frequency (RF) trap (17). We choose two ⁹Be⁺ hyperfine states, denoted $|\downarrow\rangle$ and $|\uparrow\rangle$, as our physical qubit basis states. We detect logic states by applying laser light resonant with a ⁹Be⁺ cycling transition (18). The detection laser causes ions in $|\downarrow\rangle$ to fluoresce, whereas ions in $|\uparrow\rangle$ fluoresce negligibly, allowing discrimination of logic states with high efficiency (19). Applying nonresonant laser beams BR (blue Raman) and RR (red Raman) with frequency difference $\omega_{BR} - \omega_{RR}$ equal to the $|\uparrow\rangle \leftrightarrow |\downarrow\rangle$ transition frequency ω_0 drives stimulated Raman transitions between $|\downarrow\rangle$ and $|\uparrow\rangle$. This “carrier” transition implements rotation of a single physical qubit, one of the fundamental quantum logic gates (19). The corresponding evolution is

$$\begin{aligned} |\downarrow\rangle &\rightarrow \cos\theta|\downarrow\rangle + e^{i\phi}\sin\theta|\uparrow\rangle \\ |\uparrow\rangle &\rightarrow \cos\theta|\uparrow\rangle - e^{-i\phi}\sin\theta|\downarrow\rangle \end{aligned} \quad (1)$$

where θ is proportional to the carrier drive duration and ϕ is the phase difference between the BR and RR beams at the position of the ion, referred to as the “ion phase.” For two ions, we write the ion phases ϕ_i for each ion as ϕ_1, ϕ_2 (20).

The experiments reported here use two trapped ions. The ions are strongly coupled by the Coulomb interaction, so that the motion of the ions along the axis decomposes into symmetric and antisymmetric normal modes at frequencies of 5.0 and 8.8 MHz, respectively. The wave vector difference between BR and RR lies along the trap axis, so we can drive transitions that couple the internal and motional states of the ions. Driving these transitions as described in (21), we perform the two-ion logic gate of Sørensen and Mølmer (22), which entangles the two ions. The evolution under this gate is

$$\begin{aligned} |\downarrow\downarrow\rangle &\rightarrow (|\downarrow\downarrow\rangle + i|\uparrow\uparrow\rangle)/\sqrt{2} \\ |\uparrow\uparrow\rangle &\rightarrow (|\uparrow\uparrow\rangle + i|\downarrow\downarrow\rangle)/\sqrt{2} \end{aligned}$$

$$\begin{aligned} |\downarrow\uparrow\rangle &\rightarrow (|\downarrow\uparrow\rangle + i|\uparrow\downarrow\rangle)/\sqrt{2} \\ |\uparrow\downarrow\rangle &\rightarrow (|\uparrow\downarrow\rangle + i|\downarrow\uparrow\rangle)/\sqrt{2} \end{aligned} \quad (2)$$

We can also realize the inverse of this gate by performing the gate three times in succession. In general, the evolution under the two-ion gate depends on the ion phases, but we choose a phase convention in which $\phi_1 = \phi_2 = 0$ during application of the two-ion gate, yielding the evolution of Eq. 2. This gate, in combination with single-qubit rotations, implements universal quantum logic (23), in the sense that these gates suffice to transform any superposition of the states $|\downarrow\downarrow\rangle, |\uparrow\uparrow\rangle, |\downarrow\uparrow\rangle$, and $|\uparrow\downarrow\rangle$ into any other superposition of those states.

The DFS realized here is spanned by $|\psi_{-}\rangle = (|\downarrow\uparrow\rangle - i|\uparrow\downarrow\rangle)/\sqrt{2}$ and $|\psi_{+}\rangle = (|\downarrow\uparrow\rangle + i|\uparrow\downarrow\rangle)/\sqrt{2}$, which form the basis states for our logical qubit. These states are clearly invariant under collective dephasing; the transformation $|\uparrow\rangle \rightarrow e^{i\epsilon}|\uparrow\rangle$, applied simultaneously to both ions, leaves any superposition of $|\psi_{-}\rangle$ and $|\psi_{+}\rangle$ invariant. Such collective dephasing is expected to be a major source of qubit decoherence for quantum information processing using trapped atoms. The encoding method demonstrated below reversibly transfers information between one physical qubit (one ion) and one decoherence-free logical qubit. The encoding works even if we have no information about the initial state of the physical qubit. This fact is essential for the use of our method in quantum information processing, in which the state to be encoded may be entangled with the state of another system.

To demonstrate the general character of the encoding method, we show that the encoding works for arbitrary states of form

$$|\downarrow\rangle(a|\downarrow\rangle + b|\uparrow\rangle) \quad |a|^2 + |b|^2 = 1 \quad a, b \text{ complex} \quad (3)$$

To prepare a state of this form, we first initialize the ions in the logic state $|\downarrow\downarrow\rangle$ by optical pumping. We then drive the carrier transition of Eq. 1 on both ions simultaneously, once with $\theta = \beta$, and again with $\theta = \beta$ and ϕ_1 , shifted by π . We set $\phi_2 = \alpha$ for both pulses. The final state has $a = \cos 2\beta$, $b = e^{i\alpha} \sin 2\beta$. In a classical picture of spin with $\beta = \pi/8$, the first drive takes $\downarrow\downarrow$ to $\searrow\searrow$. The second drive reverses the sense of rotation on ion 1 while keeping it the same on ion 2, so the second drive takes $\searrow\searrow$ to $\downarrow\rightarrow$. The net effect is to rotate ion 2 alone, without changing the state of ion 1 (24).

We encode the state of Eq. 3 into the DFS in two steps. First, we apply the inverse of the two-ion gate of Eq. 2, yielding $a(|\downarrow\downarrow\rangle - i|\uparrow\uparrow\rangle) + b(|\downarrow\uparrow\rangle - i|\uparrow\downarrow\rangle)$. Then, we drive the carrier with $\theta = \pi/4$, $\phi_1 = \pi/2$, $\phi_2 = 0$ to

¹Time and Frequency Division, National Institute of Standards and Technology, Boulder, CO 80305, USA.

²Department of Physics, University of Michigan, Ann Arbor, MI 48109, USA.

*To whom correspondence should be addressed. E-mail: davidk@boulder.nist.gov

obtain $|\psi_{\text{DFS}}\rangle = a|\psi_+\rangle + b|\psi_-\rangle$. The information stored in the physical qubit of ion 2 is now encoded in the logical qubit of the DFS. In the experiment, we take $|a| = |b|$, though our method permits preparation and encoding of any state of the more general form.

To read out the encoded information, we reverse the carrier pulse in the encoding and apply the two-ion gate of Eq. 2 to decode $|\psi_{\text{DFS}}\rangle$ into $|\downarrow\rangle(a|\downarrow\rangle + b|\uparrow\rangle)$. After decoding, we rotate ion 2 as in preparing the state of Eq. 3 but with the phase on ion 2 changed to α' . We then measure the probability P_2 of finding both ions in $|\downarrow\rangle$. P_2 varies sinusoidally with $\alpha - \alpha'$, and the magnitude of oscillation is equal to the coherence C of ion 2 (25). Because we set $|a| = |b| = 1/\sqrt{2}$, ideally $C = 1$. Departures from $C = 1$ measure the effects of both decoherence and imperfect logic. We verified that C is independent of α , thus showing that our encoding method works even if we have no information about the phase of the input state.

To study the effects of decoherence on the DFS-encoded state, we leave a fixed delay time between the encoding and decoding steps and apply an engineered noisy environment for some fraction of the delay time. The engineered environment consists of an off-

resonant laser beam with a randomly varying intensity. The beam induces a shift of ω_0 through the ac Stark effect, causing the $|\uparrow\rangle$ component of each ion to acquire a random phase relative to the $|\downarrow\rangle$ component. The two ions are nearly equally illuminated by the beam, so the random phase is nearly the same on both ions, leading to collective dephasing. The DFS state should resist the dephasing effect of this environment. The coherence of ion 2 in the test state $(|\downarrow\rangle(|\downarrow\rangle + e^{i\phi}|\uparrow\rangle)/\sqrt{2})$, however, should be sensitive to collective dephasing. We measure the decay of the test state by simply turning off the encoding and decoding sequences in the procedure used to measure the decay of the DFS-encoded state.

We applied decoherence to the test and encoded states during a delay time of $\sim 25 \mu\text{s}$ (Fig. 1). The coherence without applied noise is ~ 0.69 for the test state and ~ 0.43 for the encoded state; they depart from 1 because of imperfect logic gates and detection, due in part to laser intensity fluctuations and heating of the ions (17, 21). For white-noise intensity fluctuations of the Stark-shifting beam, we expect C to decay exponentially for the test state, as shown by the fit line. The small decay rate of the test state between 0 and 2.5- μs noise duration arises because the in-

tensity fluctuations of the noise beam have finite bandwidth (dc to 100 kHz) (6). We therefore extract the decay rate of the test state by excluding the point with zero applied noise from the fit. We also fit the coherence of the DFS state to an exponential decay for comparison. The decay rate of the test state is $0.18 \pm 0.01 \mu\text{s}^{-1}$, whereas the decay rate of the DFS state is $0.0035 \pm 0.0050 \mu\text{s}^{-1}$, consistent with zero decay. To investigate the eventual decay of the DFS state, we increased the delay time to $\sim 200 \mu\text{s}$ and applied decoherence for up to 100 μs during the delay time. The DFS state coherence dropped by 50% for 100- μs applied noise relative to its value for the same delay time and no applied noise, but we think that this decay was not due to collective dephasing. The decay was Gaussian, rather than exponential, and is consistent with the effect of differential dephasing due to small departures from equal illumination by the Stark-shifting beam. We think that ambient sources of differential dephasing are much weaker than the differential dephasing caused by the Stark-shifting beam.

We also measured the storage times of the encoded and test states under ambient conditions in our laboratory (Fig. 2). Here we measure the coherence as a function of the delay time between encoding and decoding to give the ambient noise a variable time to act, rather than leaving a fixed delay time and applying noise for some fraction of the delay time. The coherence data for this case are normalized in the same way as the data with applied noise. The decoherence of the test state is dominated by ambient fluctuating magnetic fields whose frequencies lie primarily at 60 Hz and its harmonics. These fields randomly shift ω_0 through the Zeeman effect. Because these fields are roughly uniform across the ion string, they induce collective dephasing similar to that created by the engineered environment. We empirically find the decay of both test and encoded states to be roughly exponential, as indicated by the fit lines. The decay rate of the test state is $(7.9 \pm 1.5) \times 10^{-3} \mu\text{s}^{-1}$, whereas the decay rate of the DFS state is $(2.2 \pm 0.3) \times 10^{-3} \mu\text{s}^{-1}$. Although Fig. 1 presents only normalized contrasts, the data show that the unnormalized contrast of the DFS state is higher than that of the test state for delay times exceeding 150 μs . The DFS-encoded state maintains coherence much longer than the test state, so we conclude that collective dephasing from magnetic field noise is the major ambient source of decoherence for the test state (26). The loss of coherence of the encoded state is consistent with degradation of the decoding pulses (19, 22, 27), due to heating of the ion motional state over the delay time (17).

We have demonstrated reversible encoding of a qubit stored in one ion into a DFS of

Fig. 1. Decay of the DFS-encoded state (circles) and the test state (crosses) under engineered dephasing noise. The noise is applied for a fraction of the delay time of $\sim 25 \mu\text{s}$ between encoding and decoding. Coherence data are normalized to their values for zero applied noise. The fit lines are exponential decay curves. The test data are predicted to decay exponentially for white noise, so we exclude the point with zero applied noise from the fit. The DFS data are fit for comparison. The decay rate of the test state is $0.18 \pm 0.01 \mu\text{s}^{-1}$, whereas the decay rate of the DFS state is $0.0035 \pm 0.0050 \mu\text{s}^{-1}$, consistent with zero decay.

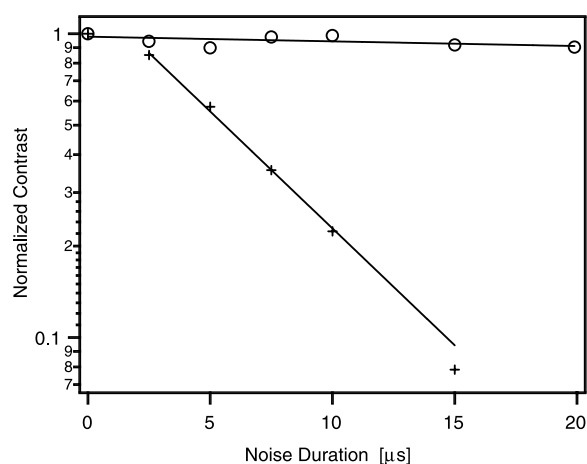
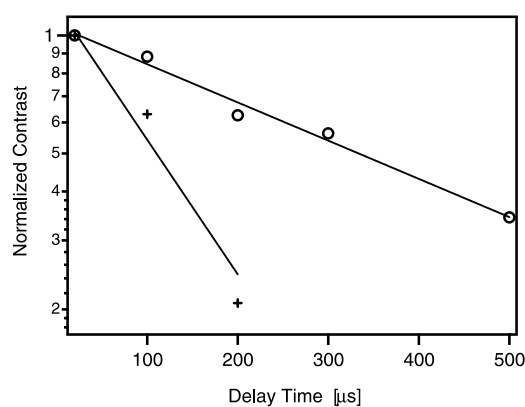


Fig. 2. Decay of the DFS-encoded state (circles) and the test state (crosses) under ambient decoherence. We vary the delay time between encoding and decoding to give the ambient noise a variable time to act. Coherence data are normalized to their values for zero applied noise. The fit lines are exponential decay curves for purposes of comparison and are not theoretical predictions. The decay rate of the test state is $(7.9 \pm 1.5) \times 10^{-3} \mu\text{s}^{-1}$, whereas the decay rate of the DFS state is $(2.2 \pm 0.3) \times 10^{-3} \mu\text{s}^{-1}$. Because the coherence time of the DFS-encoded state is much longer than that of the test state, we see that the chief source of ambient decoherence is collective dephasing.



two ions. The DFS-encoded state can store a qubit at least 10 times as long under applied noise as a single ion can, and appears immune to collective dephasing. Under typical ambient conditions, the DFS encoding also improves storage time considerably, showing that collective dephasing is indeed the limit to quantum memory using our physical qubits. Even without normalizing for the overhead incurred in encoding and decoding, the encoded state retains more coherence than the test state for long storage times in ambient conditions. The DFS encoding therefore currently provides an improved single-qubit quantum memory for ion-trap quantum computing applications. The loss of coherence incurred in encoding and decoding is a drawback to our scheme, but in the future, practical quantum computing will in any case require logic gates of a much higher fidelity than those used in this work. We therefore expect that, once the technical problems of ion heating and laser fluctuations are solved, the scheme presented here should be a practical method for long-term storage of qubits with near-perfect fidelity.

Our results suggest applications in quantum communication and large-scale quantum computing. Single photons have already been shown to transmit quantum information over long distances with high fidelity (8, 9), and the information in a single photon can be mapped onto a single atom (28, 29). With our encoding technique, the quantum information received by a single ion can be mapped into a DFS for robust storage. Our encoding technique will also be essential in scaling up ion-trap quantum computers. In one model of large-scale ion-trap quantum computing (19), qubits reside in a large array of interconnected ion traps. To perform one- or two-qubit logic gates, the relevant ions are moved into "accumulator" regions where they interact with lasers that drive the gates. One obstacle to this quantum computing architecture is that the magnetic field strength must be well-characterized across the entire device. Otherwise, the ions will constantly accumulate unknown relative phase during transport, leading to decoherence. Encoding into the DFS solves this problem, because the phase of a logical qubit in the DFS does not depend on the local magnetic field strength as long as the field strength is the same at each physical qubit. Thus, we can entangle two logical qubits, move them far apart, and perform operations on them in separate accumulators without losing phase information.

References and Notes

1. P. W. Shor, in *Proceedings of the 35th Annual Symposium on Foundations of Computer Science*, S. Goldwasser, Ed. (IEEE Computer Society, Los Alamitos, CA, 1994), p. 116.
2. L. K. Grover, *Phys. Rev. Lett.* **79**, 325 (1997).
3. A. Steane, paper presented at the Fifth International

Conference on Quantum Communication, Measurement, and Computing, Capri, Italy, 3 to 8 July 2000.

4. W. H. Zurek, *Phys. Today* **44** (no. 10), 36 (1991).
5. D. Giulini *et al.*, *Decoherence and the Appearance of a Classical World in Quantum Theory* (Springer, Berlin, 1996).
6. G. M. Palma, K.-A. Suominen, A. K. Ekert, *Proc. R. Soc. London Ser. A* **452**, 567 (1996).
7. P. Zanardi, F. Rossi, *Phys. Rev. Lett.* **81**, 4752 (1998).
8. *Fortschr. Phys.* **46** (no. 4-8) (1998).
9. *Fortschr. Phys.* **48** (no. 9-11) (2000).
10. D. A. Lidar, I. L. Chuang, K. B. Whaley, *Phys. Rev. Lett.* **81**, 2594 (1998).
11. P. Zanardi, M. Rasetti, *Phys. Rev. Lett.* **79**, 3306 (1997).
12. L. M. Duan, G. C. Guo, *Phys. Rev. A* **57**, 737 (1998).
13. D. A. Lidar, D. Bacon, K. B. Whaley, *Phys. Rev. Lett.* **82**, 4556 (1999).
14. D. Bacon, J. Kempe, D. A. Lidar, K. B. Whaley, *Phys. Rev. Lett.* **85**, 1758 (2000).
15. A. Beige, D. Braun, B. Tregenna, P. L. Knight, *Phys. Rev. Lett.* **85**, 1762 (2000).
16. P. G. Kwiat, A. J. Berglund, J. B. Altepeter, A. G. White, *Science* **290**, 498 (2000).
17. Q. A. Turchette *et al.*, *Phys. Rev. A* **61**, 063418 (2000) (available at <http://publish.aps.org/abstract/PRA/v61/e063418>).
18. The hyperfine states corresponding to $|\downarrow\rangle$ and $|\uparrow\rangle$ are the $|F = 2, m_F = -2\rangle$ and $|F = 1, m_F = -1\rangle$ sublevels of the ground $^2S_{1/2}$ state, respectively. The cycling transition is excited by left circularly polarized light and connects $|\downarrow\rangle$ to the $|F = 3, m_F = -3\rangle$ sublevel of the excited $^2P_{3/2}$ state.
19. D. J. Wineland *et al.*, *J. Res. NIST* **103**, 259 (1998).
20. For two ions, we effect common-mode changes of ϕ_1 and ϕ_2 by changing the phase of the RF synthesizer that controls the difference frequency $\omega_{BR} - \omega_{RR}$. By changing the oscillation frequency of the trap, we can control the ion spacing precisely, allowing us to make differential changes to ϕ_1 and ϕ_2 . These two techniques combined allow us to control ϕ_1 and ϕ_2 independently for two ions.
21. C. A. Sackett *et al.*, *Nature* **404**, 256 (2000).
22. A. Sørensen, K. Mølmer, *Phys. Rev. A* **62**, 022311 (2000) (available at <http://publish.aps.org/abstract/PRA/v62/e022311>).
23. _____, *Phys. Rev. Lett.* **82**, 1971 (1999).
24. Individual optical addressing of the ions can prepare

the desired state with only one carrier pulse [H. C. Nägerl *et al.*, *Phys. Rev. A* **60**, 145 (1998)], but it is technically more challenging in our experiment because our ions are separated by only $\sim 2.5 \mu\text{m}$.

25. The decoding and final rotation can give rise to coherence in ion 2 even if the state before decoding is completely incoherent. We avoid this eventuality by detuning the RF synthesizer used for the initial and final rotations of ion 2 from the synthesizers used for encoding and decoding. The phases α and α' then change from shot to shot of the experiment, and the spurious coherences average out over many shots. No trace of this effect then remains in the data.
26. We can also reduce the dephasing from this mechanism by using the $^2S_{1/2}$ hyperfine sublevels $|F = 1, m_F = 0\rangle$ and $|F = 2, m_F = 0\rangle$ to represent the two levels of a qubit. In a separate experiment, we measured the coherence time of superpositions of these two states at a static magnetic field of $\sim 1.6 \times 10^{-3}$ T to be an order of magnitude longer than the coherence time between the qubit basis states used here. Magnetic field dephasing still limits the coherence time between the $m_F = 0$ states through the quadratic Zeeman shift. We expect the DFS encoding to improve coherence time in this case as well, because the encoding protects against purely collective dephasing to all orders. A practical ion-trap quantum computer will probably use the $m_F = 0$ states as qubit basis states but will also encode qubits into the DFS.
27. B. E. King *et al.*, *Phys. Rev. Lett.* **81**, 1525 (1998).
28. X. Maitre *et al.*, *Phys. Rev. Lett.* **79**, 769 (1997).
29. J. I. Cirac, P. Zoller, H. J. Kimble, H. Mabuchi, *Phys. Rev. Lett.* **78**, 3221 (1997).
30. This work was supported by the U.S. National Security Agency and the Advanced Research and Development Activity under contract MOD-7171.00 and by the U.S. Office of Naval Research. We thank J. Bergquist and A. Ben-Kish for comments on the manuscript. This paper is a contribution of the National Institute of Standards and Technology and is not subject to U.S. copyright.

10 November 2000; accepted 22 December 2000
 Published online 5 January 2001;
 10.1126/science.1057357
 Include this information when citing this paper.

Magnetization Precession by Hot Spin Injection

W. Weber,^{1*} S. Riesen,¹ H. C. Siegmann²

As electrons are injected at various energies into ferromagnetic material with their spin polarization vector perpendicular to the axis of the magnetization, we observe precessional motion of the spin polarization on the femtosecond time scale. Because of angular momentum conservation, the magnetization vector must precess as well. We show that spin injection will generate the precessional magnetization reversal in nanosized ferromagnetic bits. At reasonable injected current densities this occurs on the picosecond time scale.

Electrons injected into ferromagnetic material experience exchange coupling to the magnetization and spin-dependent scattering, leading to excitations of the magneti-

zation (1-4). By injecting currents of high density, these excitations have been observed through the occurrence of spin waves (5-7), permanent changes of the micromagnetic structure (8, 9), or even a reversal of the magnetization (10-12). However, to date, the injection of electrons from a ferromagnetic emitter through nanocontacts occurs continuously or in pulses that are long compared with the relaxation

¹Laboratorium für Festkörperphysik, ETH Zürich, CH-8093 Zürich, Switzerland. ²Stanford Linear Accelerator Center, Stanford University, Stanford, CA 94309, USA.

*To whom correspondence should be addressed. E-mail: weber@solid.phys.ethz.ch